NASA TN D-928

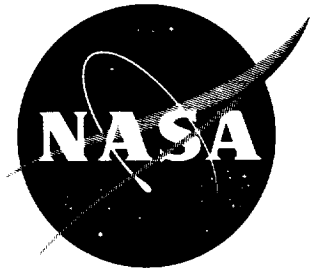

TECHNICAL NOTE

D-928

EFFECTS OF CONSTITUENT PARTICLES ON THE NOTCH-SENSITIVITY AND FATIGUE-CRACK-PROPAGATION CHARACTERISTICS OF ALUMINUM-ZINC-MAGNESIUM ALLOYS

By Larry H. Glassman and Arthur J. McEvily, Jr.

Langley Research Center
Langley Station, Hampton, Va.

NATIONAL AERONAUTICS AND SPACE ADMINISTRATION

WASHINGTON April 1962

E

NATIONAL AERONAUTICS AND SPACE ADMINISTRATION

TECHNICAL NOTE D-928

EFFECTS OF CONSTITUENT PARTICLES ON THE NOTCH-SENSITIVITY AND FATIGUE-CRACK-PROPAGATION CHARACTERISTICS OF ALUMINUM-ZINC-MAGNESIUM ALLOYS

By Larry H. Glassman and Arthur J. McEvily, Jr.

L
1
2
3
6

SUMMARY

Sheet specimens of two aluminum-zinc-magnesium alloys, 7075-T6 and X7275-T6, were tested to determine the relative sensitivity to sharp notches under static loading conditions and to determine relative resistance to fatigue crack propagation. These alloys differ chiefly with respect to the number and size of constituent particles, the level being considerably lower in the X7275 alloy. Evidence is presented which indicates that reduction in particle size and number can increase somewhat the ductility of unnotched specimens without impairing the static strength, but the material with the greater constituent-particle content was found to be more resistant to fatigue crack propagation. For both materials the sensitivity to sharp notches under static loading conditions was about the same. A discussion and interpretation of the results are given.

INTRODUCTION

The relatively high static notch sensitivity of Al-Zn-Mg alloys is a matter of concern in structural applications, especially with respect to failure due to the presence of fatigue cracks. The cause of this notch sensitivity is not readily apparent because of complicated interaction effects between such factors as lattice distortion, grain size, chemical composition, and the size and distribution of constituent particles. The purpose of the present paper is to assess the influence of the size and distribution of constituent particles on notch sensitivity and on the rate of fatigue crack propagation.

SYMBOLS

K_t	theoretical stress concentration factor
K_u	ratio of S_u to S_{nu}
R	ratio of minimum stress to maximum stress in load cycle
S_o	maximum cyclic stress based on initial net section, ksi
S_{nu}	maximum load in static fracture test divided by the net section area immediately prior to the static fracture test, ksi
S_u	ultimate tensile strength, ksi
S_y	yield stress (0.2 percent offset), ksi
ρ'	Neuber material constant, in.
ρ_e	effective radius of fatigue crack, in.

GENERAL BACKGROUND

In the course of work on the fracture characteristics of high-strength aluminum alloys 2024-T3 and 7075-T6, it was noticed that cracks were present in the constituent particles of as-received material. These cracked particles were located in the interior of the sheet, and typical examples are shown in figure 1. Since these cracks were always perpendicular to the rolling direction, it appeared that the cracks were formed during the rolling process. In sheet specimens of thickness near 0.1 inch, the material near the center plane was typical of 90 percent of the entire thickness. Particles located at the surface generally did not contain these cracks, and these particles were smaller than in the interior, as shown in figure 2.

In order to determine whether additional cracks could be introduced by deformation, a number of specimens were stretched in either the rolling or the transverse direction. After a plastic strain of 3 to 5 percent, cracks were found in both surface and interior particles. These cracks ran perpendicular to the direction of strain (fig. 3), and in some particles cracks due to rolling and the subsequent transverse strain appeared at right angles to each other, as shown in figure 4. Cracks were not detected for strains of less than 3 percent.

The constituent particles in which these cracks appear are complex intermetallic compounds, roughly platelike in shape, with the maximum dimension ranging up to 25 microns. They are much harder than the surrounding matrix and because of their brittle nature they lack the ability to accommodate large strains and so must either separate from the matrix or fracture during plastic elongation. From the work of Donnell (ref. 1) on stress concentrations at discontinuities, it might be expected that separation should occur at the interface between particle and matrix. In fact, Puttick (ref. 2) has given examples of this type of behavior for copper oxide particles in a copper matrix. However, no such separation was found in the present investigation, which indicates that the tensile strength of the constituent particle is less than the strength of the interface in high-strength aluminum alloys.

As plastic deformation continues beyond the point of crack formation, the cracks develop into voids, with the process of void formation being most pronounced at clusters of cracked particles located within the necked-down region of the specimens, as shown in figures 5 and 6. Rogers (ref. 3) has shown that void formation is a preliminary step in ductile fracture. These results indicate that the fracture is initiated at the cracked particles, and they further suggest that fracture might be delayed - that is, greater elongation prior to fracture would take place - if the large particles were eliminated. In fact, Cottrell (ref. 4) suggests that the interior voids, which appear during ductile failure, always start at inclusions and that, if material were inclusion free, failure would be due to the inward growth of the external neck, giving nearly 100 percent reduction of area.

In addition to possible effects on ductility, the constituent particles might also affect the notch sensitivity of the material inasmuch as the stress concentrating effect of cracked particles located in the vicinity of a notch or crack would aggravate the stress condition and hasten the onset of complete fracture. Such local stresses might also influence the rate of fatigue crack propagation.

In order to determine the influence of constituent particles on ductility, fracture, and fatigue crack propagation, two high-strength aluminum alloys, differing chiefly in constituent particle content, were investigated. The results of this investigation are described in the present paper.

MATERIALS, SPECIMENS, AND TESTS

Materials and Properties

The materials examined in this investigation were sheet specimens of 7075-T6 and X7275-T6 aluminum alloys. The 7075-T6 material was obtained from stock and two thicknesses were used, 0.063 and 0.093 inch. The X7275-T6 material was supplied by the Aluminum Company of America in the form of sheets $11\frac{1}{2}$ inches wide by 24 inches long by 0.093 inch thick.

The composition and heat treatment of the 7075-T6 and X7275-T6 materials are given in tables 1 and 2. The principal difference between these two alloys is the lower iron and silicon content of the X7275-T6. Photomicrographs of the surface and interior of these materials are shown in figures 7 to 14. The smaller size and number of constituent particles in the X7275-T6 alloy are apparent from these figures.

Typical stress-strain curves obtained in this investigation for each of these materials are shown in figure 15. The mechanical properties of the alloys are listed in table 3.

Specimens

Two types of specimens in three widths were tested in order to evaluate the notch sensitivities of the alloys. One type of specimen contained an internal notch of 0.005-inch radius. The other type of specimen contained a fatigue crack which was grown from an internal notch. Specimen configurations are shown in figure 16.

Notches were prepared by first cutting to within approximately 0.030 inch of the desired length of cut with a fine jeweler's saw. The 0.005-inch-radius notches were then formed by repeatedly drawing a nylon thread impregnated with a fine grinding compound across the notch. The fatigue crack notches were formed by growing fatigue cracks from these thread-cut notches in axial load under alternating tension at an initial, arbitrary, maximum, cyclic, stress level of 13,000 psi.

In most of the tests, the tip-to-tip length of the internal notches was about 30 percent of the total width in order to obtain a maximum value for the stress concentration factor. In a few cases notches of length other than 30 percent of specimen width were used in order to investigate the effect of notch length on notch sensitivity. Details of the specimen configurations together with the theoretical stress concentration factors for notched specimens are given in table 4.

Tests

The strength of specimens containing internal notches was determined by static tensile testing in a hydraulic testing machine. The strain rate in these tests was approximately 0.002 per minute.

Additional tests were made on 2-inch-wide specimens in order to determine the relative rate of fatigue crack propagation in these materials. Specimens were loaded in tension at an initial, maximum, cyclic, stress level of 13,000 psi with R = 0. Constant loading amplitude was maintained until failure. In these tests, the region of the specimen in the vicinity of the notch was polished in order to facilitate observation of the fatigue crack as it grew, and cracks were started from a 0.125-inch-long thread-cut stress raiser. Scribe marks were placed perpendicular to the path of the crack at 0.100-inch intervals. Growth of the crack was observed during alternating tension loading of the specimen by means of a 30-power microscope and stroboscopic illumination.

Upon completion of the tests, small samples were cut from the test specimens in regions of interest and polished with magnesium oxide powder for metallurgical examination.

RESULTS AND DISCUSSION

The results of the tensile tests on notched specimens are presented in figure 17 in terms of the ratio of the net section stress at failure to the ultimate tensile strength of the material. For comparison, theoretical curves computed for 7075-T6 as in reference 5 are also shown in figure 17. The net section width is defined as the total width minus the tip-to-tip length of the internal notch or fatigue crack which existed prior to tensile testing to failure. Individual test results are given in table 4.

In the fatigue-crack-propagation tests the cracks grew symmetrically from each side of the stress raiser. The results of the tests are given in table 5 and the average values for the two tests of each material are shown in figure 18.

Stress-Strain Tests

The stress-strain curves shown in figure 15 for these materials indicate that the X7275-T6 alloy has greater ductility as measured in terms of elongation than does the 7075-T6 alloy and that no sacrifice in strength is made to achieve this ductility. In fact, the 85.9-ksi strength of X7275-T6 is somewhat greater than the strength

value associated with 7075-T6. This increase in ductility may be of significance in forming operations where large plastic deformation without cracking is required. These results are in accord with the concept that the elimination of premature void formation by removing large constituent particles at which voids form will allow greater elongation prior to failure.

Observations of regions such as those shown in figures 7 to 14 bring out another important point concerning the processes leading to fracture, which is that the distribution of the constituent particles also influences the fracture process. The particles are not uniformly distributed throughout the 7075-T6 sheet but instead tend to form clusters. This clustering can accelerate fracture because it facilitates the linking up of individual voids. Void formation is also of interest concerning the onset of necking. Since the voids form and join before necking sets in and since necking occurs sooner in 7075-T6 than in X7275-T6, it is considered that void formation accelerates the process of necking. The high hydrostatic tensile stresses developed during necking serve to open voids still further.

In addition to their effect on void formations, clusters of constituent particles also retard grain growth, because in the vicinity of such clusters in 7075-T6 the grain size is smaller than in regions relatively free of such particles, as shown in figure 19.

Residual Static Strength

Examination of figure 17 reveals that for 11-inch-wide specimens there is no significant difference between the notch sensitivity of X7275-T6 and 7075-T6. In these specimens the fatigue cracks exhibited about the same severity as stress raisers as did the 0.005-inch notches.

The data points for the 2-inch-wide specimens are grouped rather closely together, indicating from a limited number of tests no significant differences between the two materials as to notch sensitivity. In these tests the fatigue cracks did appear to be slightly more severe as stress raisers than the 0.005-inch notches though the difference was not significant.

The data points for the $2\frac{1}{2}$-inch-wide specimens indicate that the X7275-T6 material is much less notch sensitive than the 7075-T6 material tested. However, in this instance the 7075-T6 alloy had a tensile strength of 87.9 ksi as compared with the nominal value of 81 ksi. Whether this high value of tensile strength increases notch sensitivity is worthy of further study. This 7075-T6 material was somewhat thinner (0.063 inch as compared with 0.093 inch for the other specimens), but in

view of the work of Irwin, Kies, and Smith (ref. 6) the difference in notch sensitivity cannot be accounted for on this basis because a decrease in thickness in this range should serve to reduce rather than increase the notch sensitivity of the material.

The insensitivity of the notched specimens to the size and extent of constituent particles, as indicated in these tests, may be due to the constrained and localized nature of the deformation at the tip of a notch or fatigue crack. The constraint arises because the surrounding material is still elastic, and localization of the fracture region by the notch lessens the possibility of finding a damaging particle in the critical region.

It is seen in figure 17 that the theoretical predictions are generally on the conservative side, especially for the smaller length notches in the 11-inch-wide specimens. This difference may be due to a notch strengthening effect which is most pronounced for low values of the stress concentration factor.

Fatigue Crack Propagation

The results of the fatigue-crack-propagation tests shown in figure 18 indicate that reduction of constituent particles is not beneficial in this respect. Examination of photomicrographs (figs. 20 and 21) of cracked regions indicates no great difference in the nature of fatigue crack propagation but, inasmuch as the present micrographic observations of fatigue cracks in axially loaded sheet specimens are made at arbitrary depth within the sheet, they probably do not reveal the factors accounting for the difference in the rate of fatigue crack propagation between these two materials. On the other hand, Hempel (ref. 7) has examined Al-Zn-Mg alloy sheet specimens in reversed bending. In such a case, the critical region is at the surface, and therefore micrographic observation of the surface provides a better basis for understanding fatigue-crack-propagation behavior.

Hempel found that fatigue cracks tend to grow from particle to particle; this result indicates that the increase in the tensile stress field in the vicinity of a particle affects the direction of crack propagation. In the present experiments, it was found that cracks grow more slowly in the alloy containing more constituent particles. This behavior suggests that, if a sufficiently large number of constituent particles are present and become cracked or otherwise weakened, they may act as crack arrestors and that, although the stresses due to the particle may attract the crack to the particle (as would a hole, for the cracked or otherwise weakened particles may be regions of lower stiffness approaching that of a hole in the limit), the propagation process is stopped and must be reinitiated in order to further propagate the crack. In the X7275-T6 alloy, in which

there are less particles, fewer arrests are made, and the rate of fatigue crack propagation is more rapid than in the 7075-T6 alloy.

CONCLUSIONS

As a result of studies on the effect of constituent particles in Al-Zn-Mg alloys on ductility, notch sensitivity, and fatigue crack propagation, the following conclusions are reached:

1. Constituent particles can reduce the ductility of Al-Zn-Mg alloys by facilitating the formation of voids during large-scale plastic elongation.

2. Constituent particles do not exert a strong influence on static notch sensitivity possibly because of the localized and constrained nature of the plastic deformation involved.

3. A sufficiently large number of weakened constituent particles may have a beneficial effect on fatigue crack propagation in that they can act as crack arrestors and retard the propagation of fatigue cracks.

Langley Research Center,
National Aeronautics and Space Administration,
Langley Field, Va., May 23, 1961.

REFERENCES

1. Donnell, L. H.: Stress Concentrations Due to Elliptical Discontinuities in Plates Under Edge Forces. Theodore von Kármán Anniversary Volume, C.I.T. (Pasadena, Calif.), May 11, 1941, pp. 293-309.

2. Puttick, K. E.: Ductile Fracture in Metals. Phil. Mag., ser. 8, vol. 4, no. 44, Aug. 1959, pp. 964-969.

3. Rogers, H. C.: The Tensile Fracture of Ductile Metals. Trans. Metall. Soc. of AIME, vol. 218, no. 3, June 1960, pp. 498-506.

4. Cottrell, A. H.: Theoretical Aspects of Fracture. Ch. 2 of Fracture, B. L. Averbach, D. K. Felbeck, G. T. Hahn, and D. A. Thomas, eds., The Technology Press of M.I.T. and John Wiley & Sons, Inc., c.1959, pp. 20-53.

5. McEvily, Arthur J., Jr., Illg, Walter, and Hardrath, Herbert F.: Static Strength of Aluminum-Alloy Specimens Containing Fatigue Cracks. NACA TN 3816, 1956.

6. Irwin, G. R., Kies, J. A., and Smith, H. L.: Fracture Strengths Relative to Onset and Arrest of Crack Propagation. Proc. ASTM, vol. 58, 1958, pp. 640-660.

7. Hempel, M. R.: Slip Bands, Twins, and Precipitation Processes in Fatigue Stressing. Ch. 19 of Fracture, B. L. Averbach, D. K. Felbeck, G. T. Hahn, and D. A. Thomas, eds., The Technology Press of M.I.T. and John Wiley & Sons, Inc., c.1959, pp. 376-411.

TABLE 1.- COMPOSITION OF Al-Zn-Mg ALLOYS

Element, percentage by weight	7075*	X7275†
Iron	0.70	0.03
Silicon	0.50	0.04
Copper	1.2 to 2.0	1.65
Magnesium	2.1 to 2.9	2.84
Manganese	0.30	0.30
Zinc	5.1 to 6.1	5.60
Chromium	0.15 to 0.40	0.22
Titanium	0.20	0.05
Beryllium	0.00	0.002

*Composition range and maximum content.
†Actual composition.

TABLE 2.- HEAT TREATMENT OF Al-Zn-Mg ALLOYS

Material	Solution	Precipitation
7075-T6*	870° F to 925° F	250° F for 22 to 26 hr or 210° F for 4 to 6 hr plus 315° F for 8 to 10 hr
X7275-T6	860° F	250° F for 24 hr

*Nominal heat treatment.

TABLE 3.- MECHANICAL PROPERTIES

[Average of three tests]

Material	Thickness, in.	S_y, ksi	S_u, ksi	Strain at S_u, percent	Total elongation in 2 inches, percent
7075-T6	0.064	77.0	87.9	9.5	13
7075-T6	.093	70.0	81.6	9.5	13
X7275-T6	.093	74.0	85.9	12.5	17

TABLE 4.- STATIC-STRENGTH TEST DATA FOR NOTCHED SPECIMENS

Material	Width	Thickness	S_u, ksi	Type of notch (a)	Crack length, percent of specimen width	K_t (b)	S_{nu}, ksi	K_u
7075-T6	2.00	0.093	81.6	FC	30.2	17.7	62.5	1.31
				FC	30.2	17.7	59.0	1.38
				TC	29.7	11.5	62.8	1.30
				TC	29.9	11.5	63.5	1.28
X7275-T6	2.00	0.093	85.9	FC	29.5	17.5	68.2	1.26
				FC	29.5	17.5	60.0	1.43
				TC	29.9	11.5	67.6	1.27
				TC	30.3	11.5	68.1	1.26
7075-T6	2.50	0.064	87.9	TC	31.8	12.9	58.0	1.51
				TC	33.2	13.0	54.7	1.61
				TC	33.9	13.1	60.9	1.44
				TC	34.8	13.1	56.7	1.55
X7275-T6	2.50	0.093	85.9	TC	33.6	13.0	68.4	1.26
				TC	34.0	13.1	70.5	1.22
7075-T6	11.00	0.093	81.6	TC	29.3	25.5	38.2	2.14
				TC	37.8	26.7	35.2	2.32
				FC	29.3	39.8	38.5	2.12
				FC	29.2	39.7	39.4	2.07
				TC	3.5	12.8	63.9	1.28
				TC	7.3	17.1	53.1	1.54
X7275-T6	11.00	0.093	85.9	TC	29.1	25.4	39.0	2.20
				TC	29.6	25.5	37.0	2.32
				FC	29.1	39.6	35.1	2.45
				FC	29.2	39.7	39.0	2.20
				TC	3.5	12.8	69.3	1.24
				TC	7.3	17.1	55.4	1.55

[a] TC, threadcut notch with radius = 0.005 in.; FC, fatigue crack.

[b] K_t computed as in reference 5, with $\rho' = \rho_e = 0.002$ in.

TABLE 5.- FATIGUE-CRACK-PROPAGATION DATA

Material	Width, in.	Thickness, in.	S_o, ksi	Total number of cycles to grow crack from 0.2 inch to -						Total life cycles
				$a_{0.4}$ in.	$a_{0.6}$ in.	$a_{0.8}$ in.	$a_{1.0}$ in.	$a_{1.2}$ in.	$a_{1.4}$ in.	
7075-T6	2.00	0.093	13.0	177×10^2	262×10^2	312×10^2	333×10^2	348×10^2	353×10^2	672×10^2
	2.00	.093	13.0	187	273	322	350	365	371	672
X7275-T6	2.00	0.093	13.0	108×10^2	157×10^2	186×10^2	217×10^2	238×10^2	252×10^2	401×10^2
	2.00	.093	13.0	110	142	172	203	233	243	390

[a]These values refer to the tip-to-tip length of the two cracks which grow from opposite sides of the stress raiser.

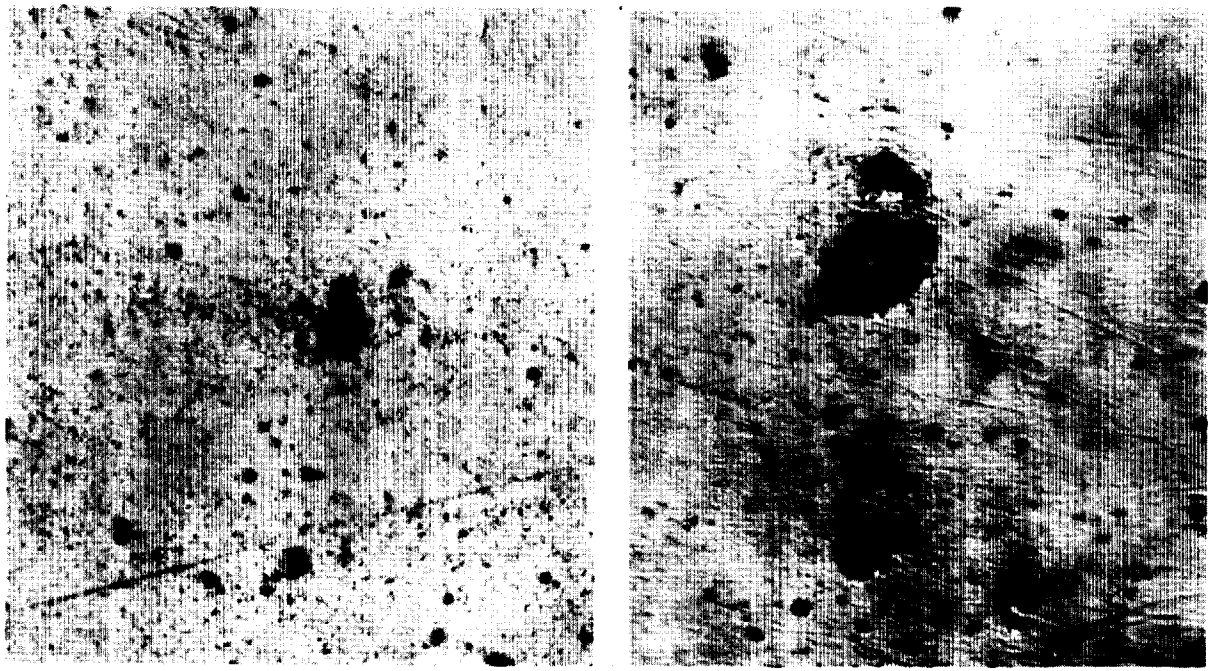

L-61-2211

Figure 1.- Cracked constituent particles in interior of 2024-T3 aluminum-alloy sheet. Rolling direction vertical (X750).

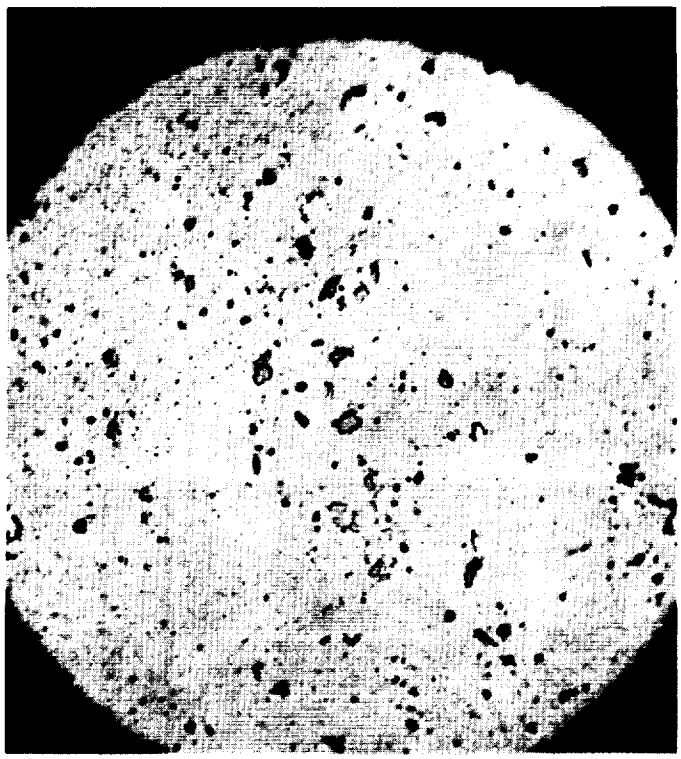

L-61-2212

Figure 2.- Constituent-particle distribution in surface of 2024-T3 aluminum-alloy sheet. Rolling direction vertical (X500).

Figure 3.- Cracks in constituent particles in 2024-T3 aluminum-alloy sheet after 5-percent extension in rolling direction. Rolling direction vertical (X500).

L-61-2213

Figure 4.- Cracks in constituent particles in 2024-T3 aluminum-alloy sheet after 5-percent extension in transverse direction. Rolling direction vertical (X500).

Figure 5.- Void formation in necked-down region at a cluster of constituent particles in 2024-T3 aluminum-alloy sheet (X500).

L-61-2214

Figure 6.- Linking of voids in necked-down region in 2024-T3 aluminum-alloy sheet (X3000).

L-61-2215

Figure 8.- Polished surface of X7275-T6 aluminum-alloy sheet (X250).

Figure 7.- Polished surface of 7075-T6 aluminum-alloy sheet (X250).

Figure 9.- Polished center plane of 7075-T6 aluminum-alloy sheet (X250).

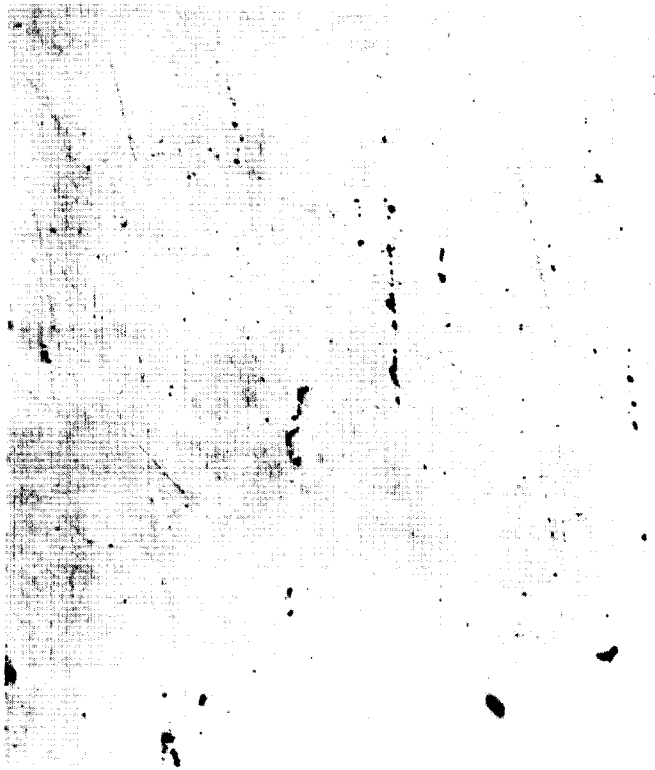

L-61-2216

Figure 10.- Polished center plane of X7275-T6 aluminum-alloy sheet (X250).

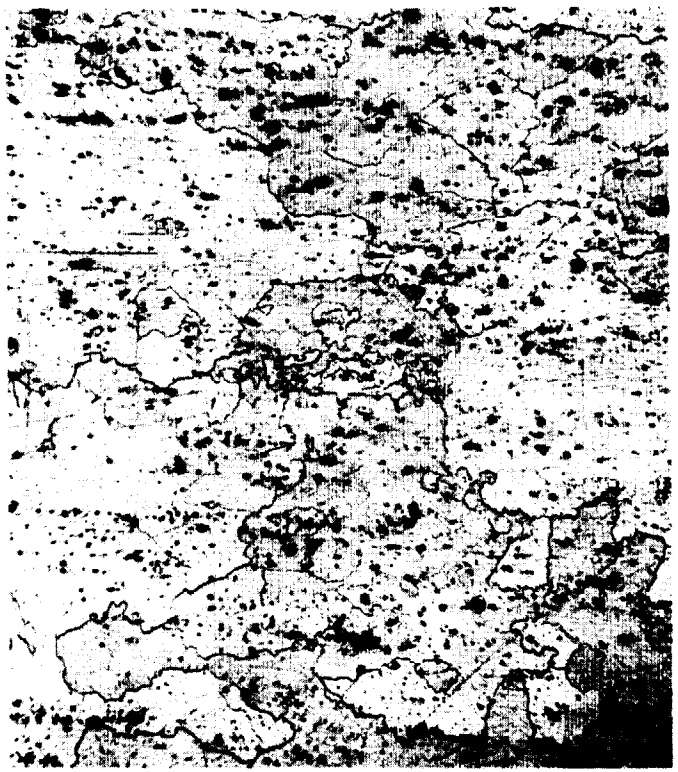

Figure 11.- Polished and etched surface of 7075-T6 aluminum-alloy sheet (X100).

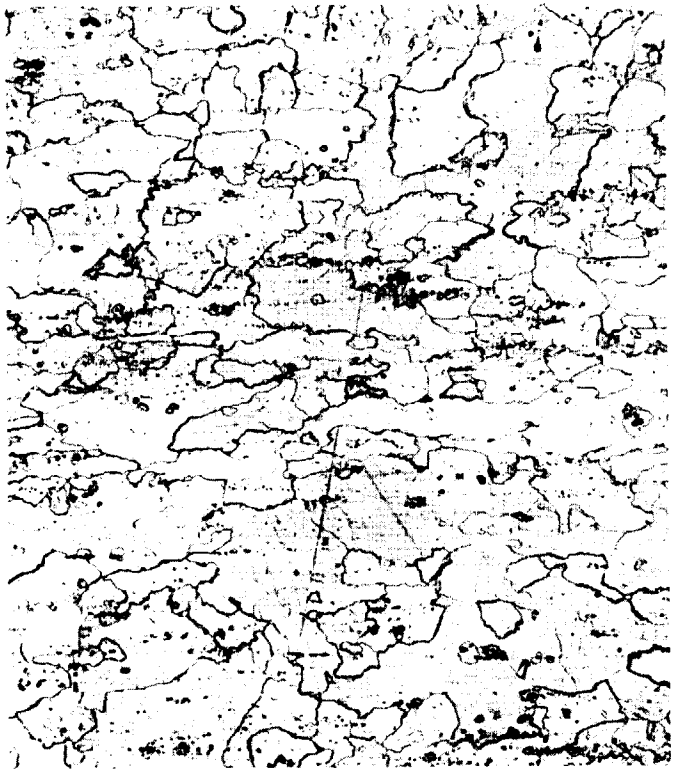

L-61-2217

Figure 12.- Polished and etched surface of X7275-T6 aluminum-alloy sheet (X100).

Figure 13.- Polished and etched center plane of 7075-T6 aluminum-alloy sheet (X100).

L-61-2218

Figure 14.- Polished and etched center plane of X7275-T6 aluminum-alloy sheet (X100).

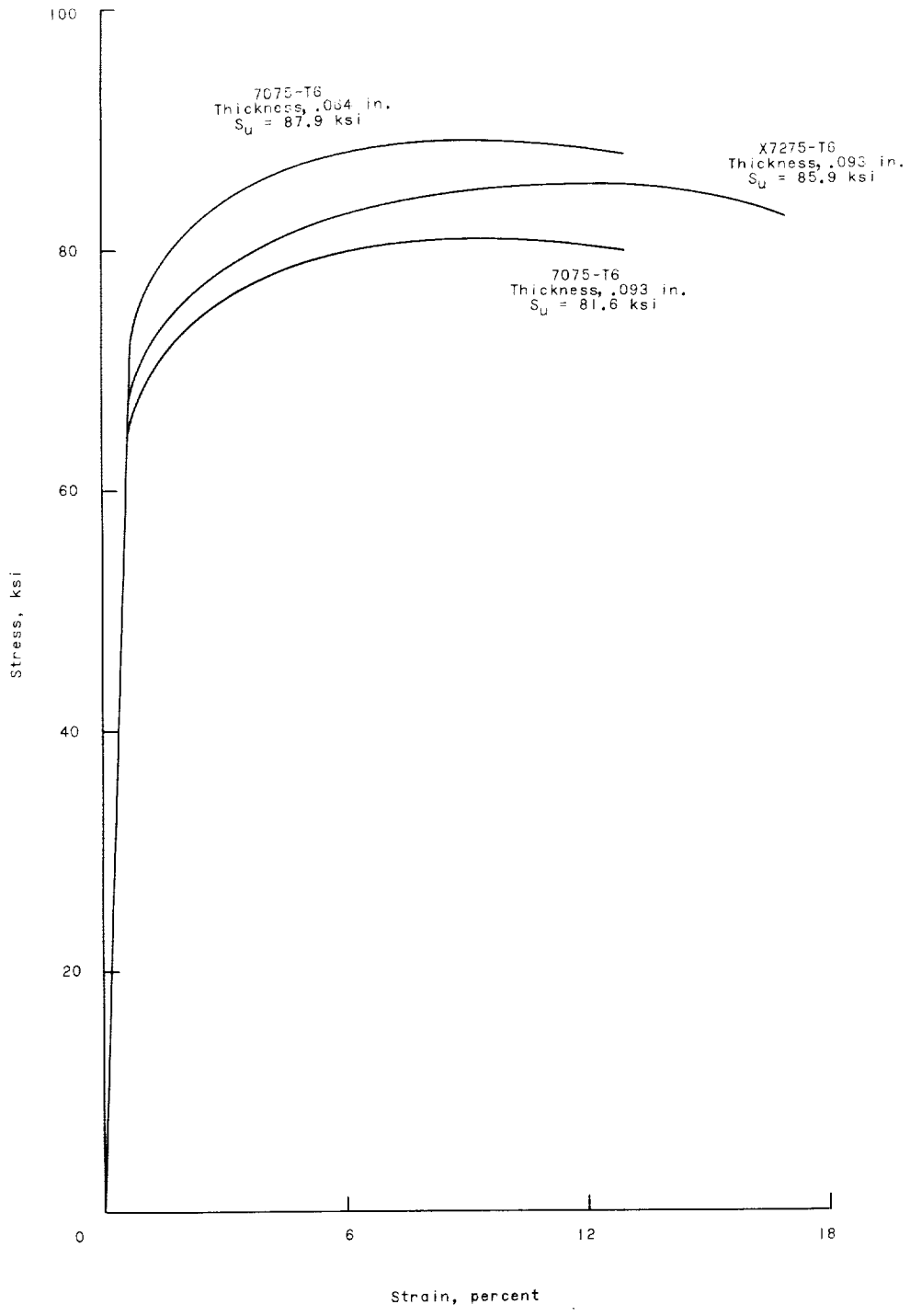

Figure 15.- Stress-strain curves for 7075-T6 and X7275-T6 aluminum alloys.

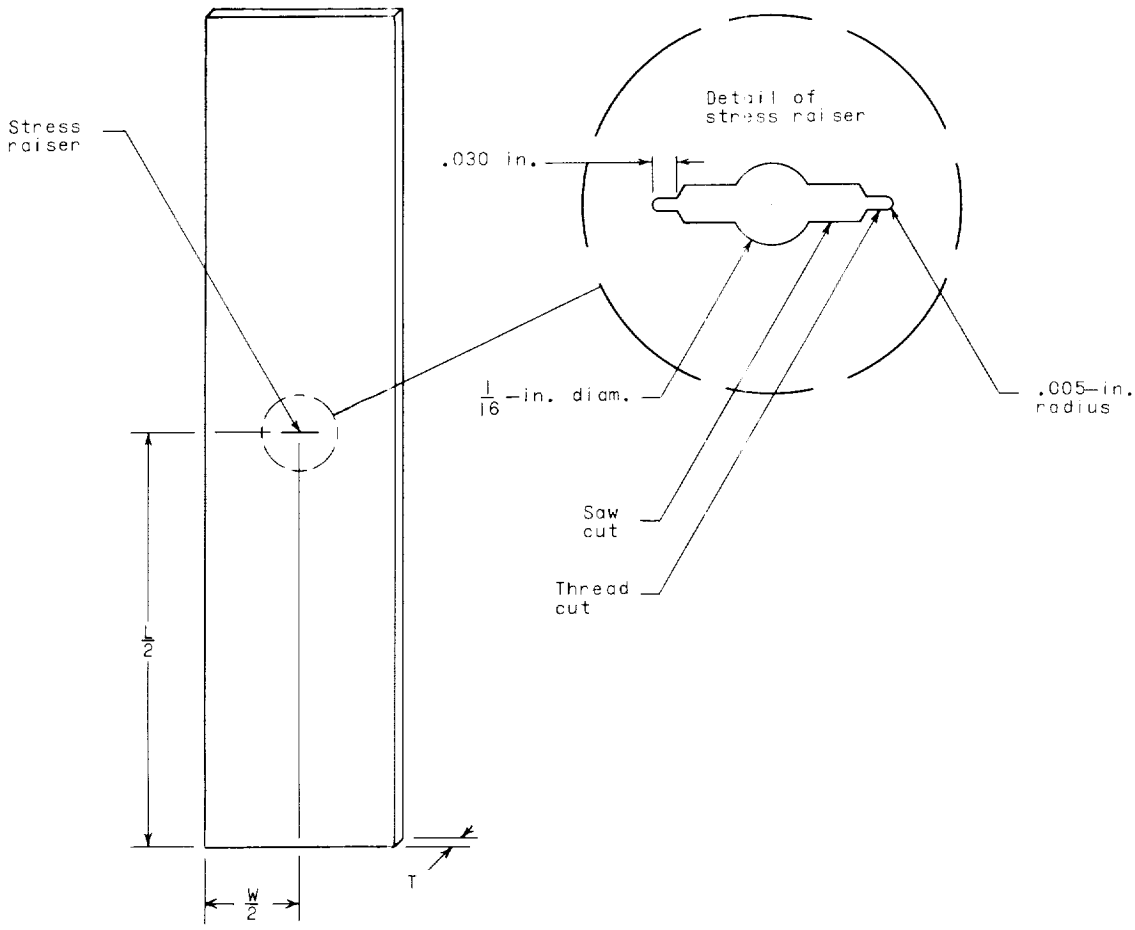

Width, W, in.	Length, L, in.	Thickness, T, in.
2.00	17.50	0.093
2.50	14.00	0.093 and 0.064
11.00	24.00	0.093

Figure 16.- Specimen configurations.

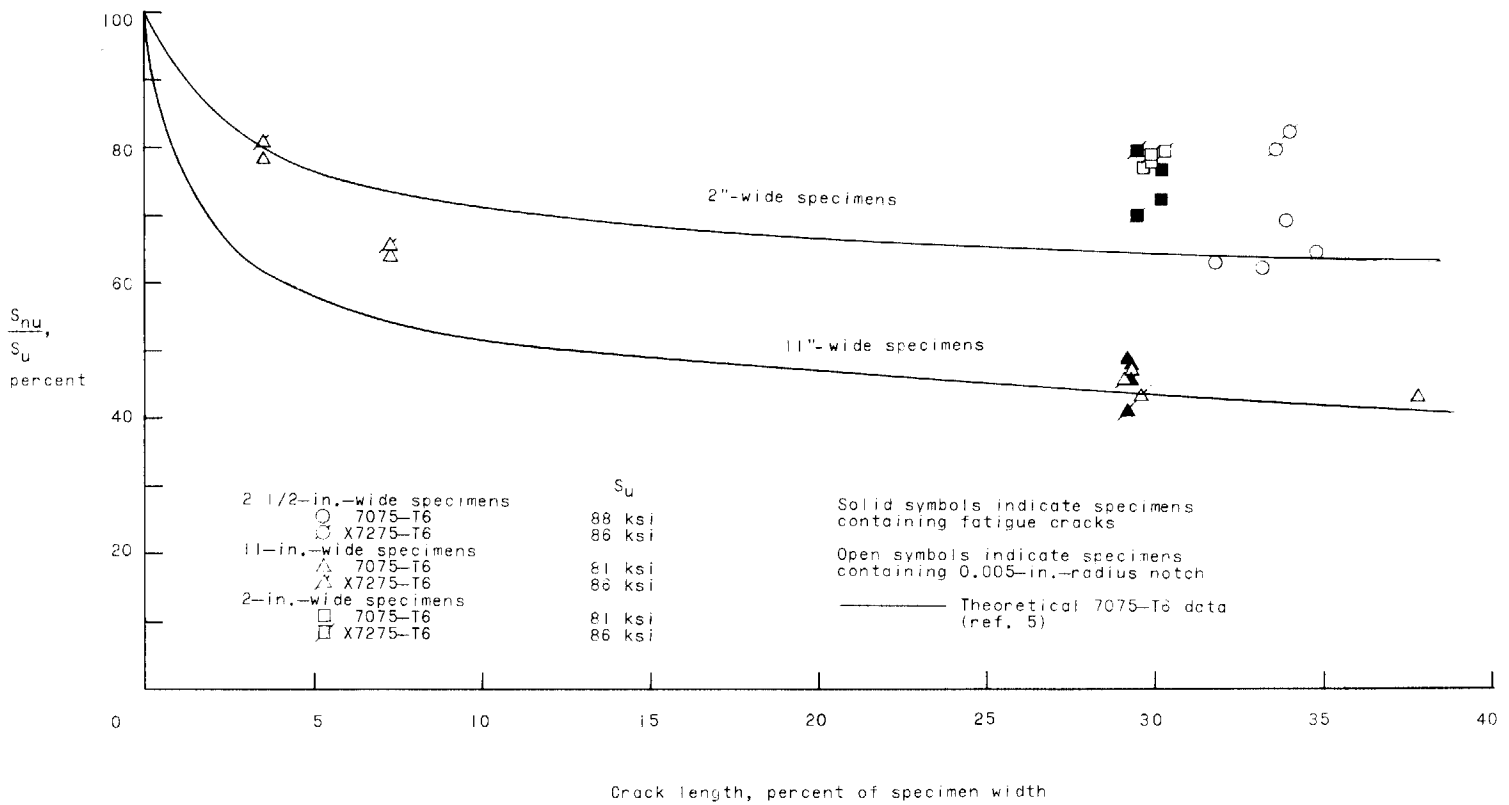

Figure 17.- Effect of stress raisers on the static strength of 7075-T6 and X7275-T6 aluminum alloys. (Curves computed for fatigue cracks in 7075-T6 as in ref. 5 with $\rho = \rho_e = 0.002$ in.)

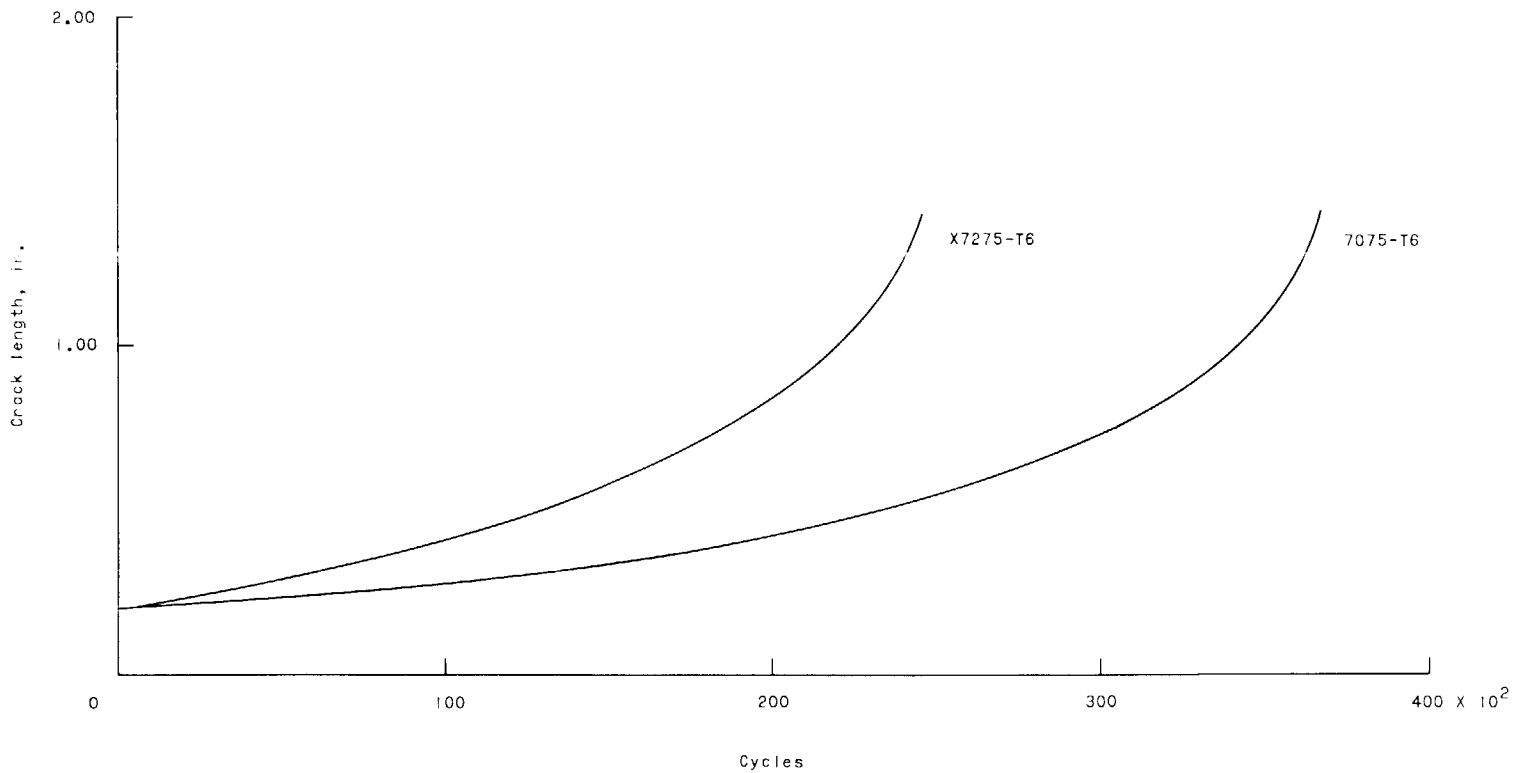

Figure 18.- Fatigue crack propagation in 7075-T6 and X7275-T6 aluminum alloys. Load amplitude held constant; R = 0.

L-1236

L-61-2219

Figure 19.- An example of the decrease in grain size in the vicinity of constituent-particle groups (X250).

NASA-Langley, 1962 L-1236

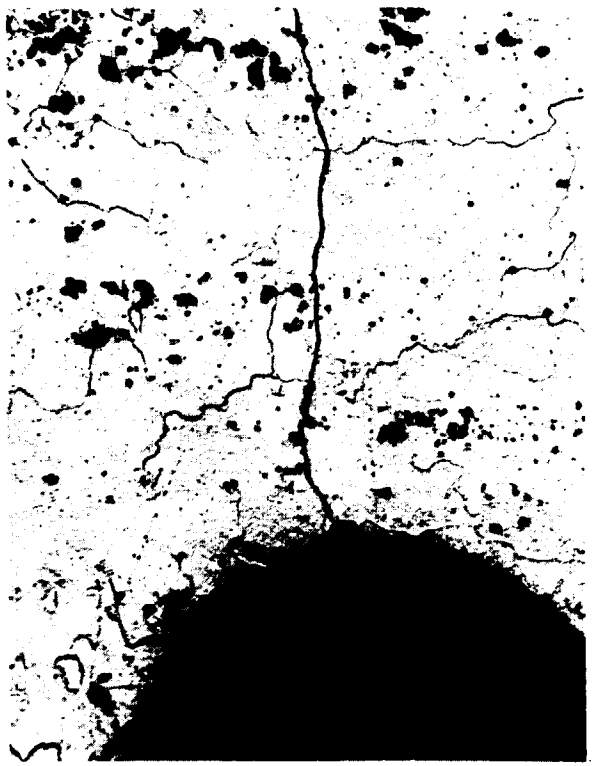

Figure 20.- Fatigue crack in center plane of 7075-T6 aluminum-alloy sheet (X250).

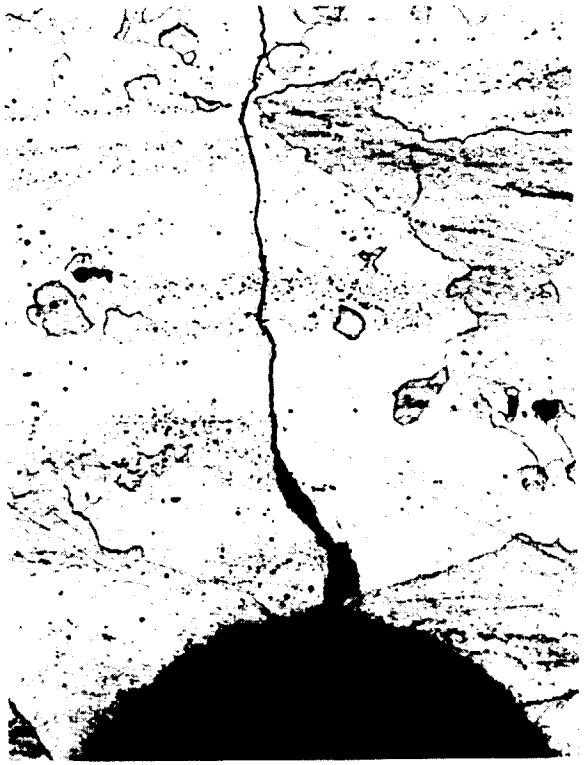

L-61-2220

Figure 21.- Fatigue crack in center plane of X7275-T6 aluminum-alloy sheet (X250).